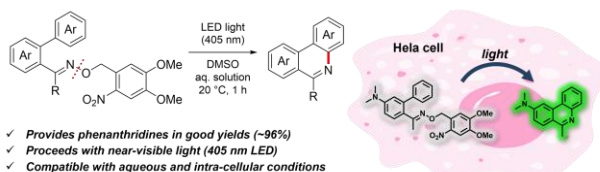


o-Nitrobenzyl oxime ethers enable photo-induced cyclization reaction to provide phenanthridines under aqueous conditions

Hidenori Okamura,^{1,2,*} Momoka Iida,^{1,2} Yui Kaneyama,^{1,2} and Fumi Nagatsugi^{1,2,*}

¹Institute of Multidisciplinary Research for Advanced Materials, Tohoku University, 2-1-1 Katahira, Aoba-ku, Sendai, Miyagi 980-8577, Japan, ²Department of Chemistry, Graduate School of Science, Tohoku University, Aoba-ku, Sendai, Miyagi 980-8578, Japan

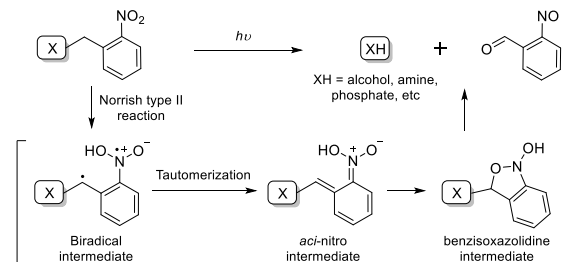


ABSTRACT: In this paper, we describe a novel N–O photolysis of *o*-nitrobenzyl oxime ethers that enables the synthesis of phenanthridines *via* intramolecular cyclization reactions. Without the use of additional photocatalysts or photosensitizers, the process proceeds with an efficiency of up to 96% when exposed to near-visible light (405 nm) under aqueous circumstances. Through the photoinduced production of a fluorescent phenanthridine derivative in HeLa cells, biocompatibility of the reaction was demonstrated. This photoinduced cyclization reaction could be used as a different photochemical instrument to control biological processes by inducing the production of bioactive molecules.

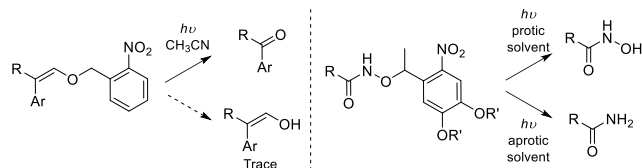
The development of photoinduced reactions that proceed under biological conditions is highly sought after for chemical biology and drug discovery studies because they offer a potent tool for perturbing and investigating biological processes in a very spatiotemporal manner.^{1–3} *o*-Nitrobenzyl moieties are representative chemical entities that can photocontrol functional molecules; these photolabile protecting groups can be covalently attached to a molecule of interest to “cage” its function, while the re-activation can be achieved on demand by photodeprotection (Fig. 1a). Since Hoffman’s first use of *o*-nitrobenzyl and its derivatives in the photocaging of ATP in 1978,⁴ they have been widely used as a photochemical handles to manipulate the bioactivity of numerous bioactive molecules.^{5–9}

The *o*-nitrobenzyl groups are typically photo-deprotected by the Norrish type II mechanism (Fig. 1a). As a result, the substituents (e.g., alcohols, amines, phosphates, etc) at the benzylic position are liberated through the formation of biradical and *aci*-nitro intermediates.^{10, 11} *o*-Nitrobenzyl moieties have also been demonstrated to exhibit several reaction modes when attached to specific chemical entities, in addition to a typical photolysis mode (Fig. 1b). For instance, Banerjee reported that *o*-nitrobenzyl enol ethers undergo C=C bond scission rather than enol-forming C–O bond cleavage upon photoirradiation and provide ketones under aerobic conditions.¹² Alternatively, Qvortrup has demonstrated that the *o*-nitroveratryl group causes solvent-dependent photolysis of hydroxylamines, providing hydroxamic acids in protic solvents or carboxamides in aprotic solvents.¹³ These investigations suggest the photoreaction modes of *o*-nitrobenzyl moieties are still unexplored and have the potential to be developed as novel photochemical instruments.

(a) *o*-Nitrobenzyl moiety as a photo-caging of bioactive compounds



(b) Unconventional reaction modes of *o*-nitrobenzyl-tethered compounds



(c) This work: Intramolecular cyclization *via* N–O photolysis of *o*-nitrobenzyl oxime ether

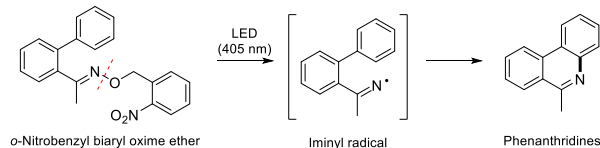


Figure 1. (a) Traditional *o*-nitrobenzyl chemistry for the photo-caging; (b) unconventional reaction modes of *o*-nitrobenzyl moieties; (c) intramolecular cyclization *via* N–O photolysis of *o*-nitrobenzyl oxime ether.

Herein, we report a novel photoreaction mode of the *o*-nitrobenzyl oxime ether. Specifically, we found that the *o*-nitrobenzyl biaryl oxime ethers undergo photoinduced N–O cleavage and produce phenanthridine derivatives *via* intramolecular cyclization (Fig. 1c). According to Scheme 1 the *o*-nitrobenzyl bi-phenyl oxime ether **3a** was synthesized from the biphenyl acetophenone **1a** and the *o*-nitrobenzyl hydroxylamine hydrochloride **2a**. Reverse phase HPLC analyses showed the simultaneous formation of two major products, when **3a** in DMSO was

exposed to a 405 nm LED light for 60 minutes under aerobic conditions (Fig. 2). A 32% yield of 6-methylphenanthridine **4a** was confirmed by spectroscopic examinations of the isolated products. In contrast, compound **5** was found to be a C–O cleaved oxime with a yield of 62% and is most likely the result of a traditional Norrish type II reaction involving the *o*-nitrobenzyl moiety.

Scheme 1. Synthesis of *o*-nitrobenzyl biaryl oxime ether.

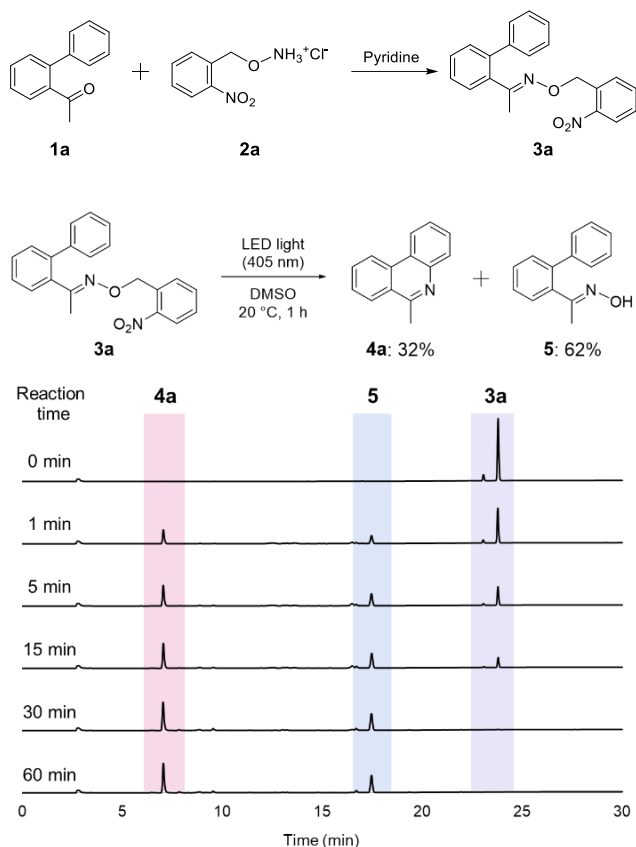


Figure 2. Formation of phenanthridine **4a** by photoirradiation of *o*-nitrobenzyl biaryl oxime ether **3a**. The Time course of the reaction was monitored by RP-HPLC over 60 min of photoirradiation (See Fig. S1 for the setup). Yields were obtained using calibration curves (Fig. S2).

Numerous synthetic methods have been reported for phenanthridine, which is one of the common structures found in biologically active compounds.^{14, 15} Recent research, in particular, showed the synthesis of phenanthridines from biaryl compounds using photosensitizers or photoredox catalysts.¹⁶⁻²¹ On the other hand, the current photoinduced reaction with *o*-nitrobenzyl oxime ether can be regarded as unique as it produces phenanthridine without any additives under near-visible light irradiation in aerobic conditions.

To further explore the reaction, we synthesized and performed the photoirradiation on the biaryl oxime ethers tethered to different *o*-nitrobenzyl derivatives as well as those with benzyl or *p*-nitrobenzyl moieties (Table 1, Fig. S3). Compared with the parental **3a** with NB group, **3b–d** bearing *o*-nitroveratryl (NV), methyl *o*-nitroveratryl (^{Me}NV), and methyl *o*-nitropiperanyl (^{Me}NP) moieties provided **4a** in higher yields of 57–66%, indicating that the methoxy or dioxolane substitution enhances the selectivity towards the phenanthridine formation.

Additionally, **3c** and **3d** demonstrated higher rate constants than **3a** and **3b**, indicating that the methyl substitution improves the reactivity. In contrast to **3a–d** bearing *o*-nitrobenzyl derivatives, **3e** and **3f** with benzyl and *p*-nitrobenzyl-substitution provided neither **4a** nor **5**. Therefore, the *o*-nitrobenzyl structure was validated to be critical as being photoinduced cyclization.

Table 1. Effect of the substituents on the *o*-nitrobenzyl moiety in the photoinduced intramolecular cyclization reaction.

Substrates		Yield of 4a (%) ^a	Yield of 5 (%) ^a	<i>k</i> (s ⁻¹)
3a: R = NB		32	62	4.7 × 10 ⁻³
3b: R = NV		57	28	7.1 × 10 ⁻³
3c: R = ^{Me} NV		66	18	3.7 × 10 ⁻²
3d: R = ^{Me} NP		61	34	1.3 × 10 ⁻²
3e: R = BN		-	-	-
3f: R = pNB		-	-	-

^aYield determined by HPLC using calibration curves.

In order to determine applicability of the photoinduced cyclization reaction in biological settings, we next investigated whether it could proceed in aqueous conditions. To achieve this, **3b** was tested for the photoinduced cyclization reaction in a mixture of DMSO and aqueous solutions (Table 2, Fig. S4). In the presence of H₂O, the HPLC analysis confirmed the formation of **4a** with a yield of 59% (Table 2, Entry 1), showing that the presence of H₂O has little effect on the reaction progress. We then investigated the reaction in the presence of an aqueous sodium phosphate buffer (10 mM, pH 7.0) instead of H₂O. Intriguingly, we found that the addition of the buffer solution significantly increases the yield of phenanthridine **4a** to 82% and quantitatively suppresses the formation of C–O cleaved oxime **5** (Table 2, Entry 2). Further investigation revealed that the reaction proceeds efficiently over a wide pH range (4.0–8.0) and is not significantly influenced by the types of buffer solutes (Table 2, Entry 3–6).

Table 2. Photoinduced intramolecular cyclization reaction in the presence of aqueous solution.^a



Entry	Aqueous solution ^a	Yield of 4a (%) ^b	Yield of 5 (%) ^b
1	H ₂ O	59	22
2	10 mM sodium phosphate buffer, pH 7.0	82	— ^c
3	10 mM sodium citrate buffer, pH 4.0	82	— ^c
4	10 mM sodium citrate buffer, pH 5.0	77	— ^c
5	10 mM sodium phosphate buffer, pH 6.0	81	— ^c
6	10 mM sodium phosphate buffer, pH 8.0	84	— ^c

^aReaction was performed in a 4:1 (v/v) mixture of DMSO and aqueous solution. ^bYield determined by HPLC using calibration curves. ^cYield not determined.

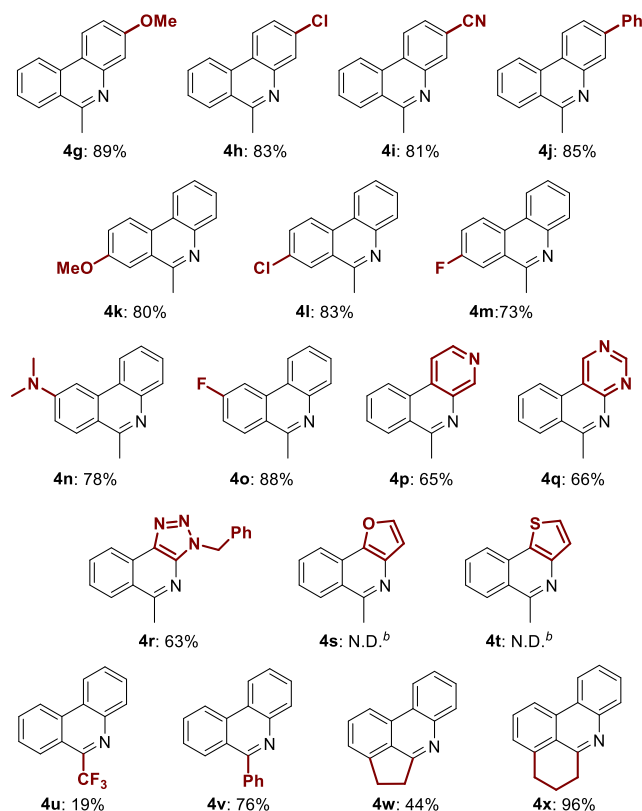
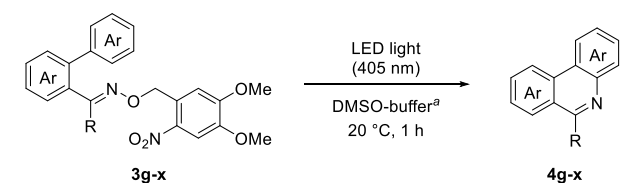
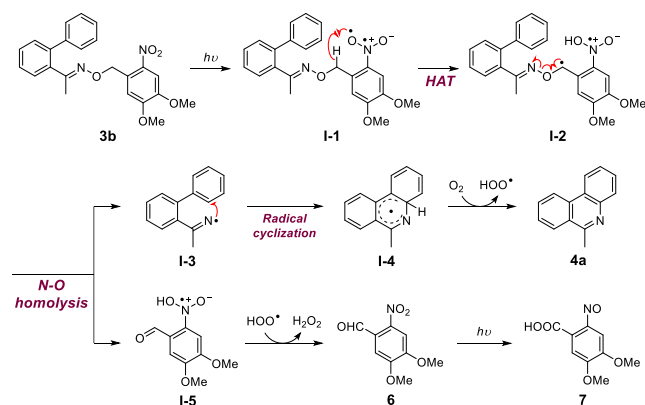


Figure 3. Substrate the scope of the photoinduced intramolecular cyclization reaction. ^a4:1 (v/v) mixture of DMSO-*d*₆ and sodium phosphate buffer (10 mM in D₂O, pH 7.0). Yields were determined by ¹H NMR using maleic acid as an external standard. ^bYield not determined.

After confirming the efficient progress of the photoinduced cyclization in aqueous solutions, we subsequently investigated the substrate scope of the reaction with a series of NV-tethered biaryl oxime ethers (Fig. 3). We discovered that the substitutions on the biaryl rings were well-tolerated; both electron-withdrawing and -donating groups on either ring of the biaryl structure afforded the corresponding phenanthridine derivatives in good yields (**4g–o**: 73–89%). The reaction also proceeded with heterocyclic biaryls to yield pyridinyl (**4p**: 65%), pyrimidinyl (**4q**: 66%), and triazolyl (**4r**: 63%) derivatives, while **4s** and **4t** bearing furanyl and thienyl moieties led to decomposition. We also examined substitution at the iminyl carbon of the oxime group; compared with the methyl-substituted compound **4a**, trifluoromethyl substitution significantly decreased the yield (**4u**: 19%), whereas phenyl substitution afforded **4v** in 76%. The reaction also proceeded with 1-indanone and 1-tetralone oxime ethers, yielding **4w** and **4x** in 44% and 96%, respectively.

We then turned our attention to the reaction mechanism. The analyses of the substrate scope demonstrated that the substituents on the iminyl carbon atom significantly influenced the reaction yield (see Fig. 3); therefore, we speculated that the iminyl radical participated in the reaction. Based on this hypothesis, we propose the reaction mechanism illustrated in Scheme 2. The *o*-nitrobenzyl moiety of **3b** is photoexcited by the 405 nm LED irradiation and forms the triplet-state biradical **I-1**. Subsequent intramolecular hydrogen atom transfer at the benzylic position produces **I-2**, which then undergoes N–O homolysis to form the iminyl radical intermediate **I-3** and *o*-nitrobenzaldehyde radical **I-5**. The iminyl radical **I-3** undergoes radical cyclization to form a cyclohexadienyl radical **I-4**, yielding phenanthridine **4a** via oxidation by O₂. The *o*-nitrobenzaldehyde **6**, which is produced simultaneously with the oxidation of **I-5**, is further photo-isomerized to produce *o*-nitrosobenzic acid **7** as a byproduct.²²

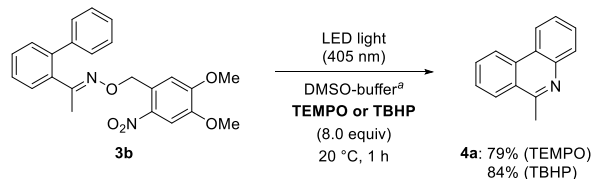
Scheme 2. Proposed reaction mechanism.



To examine the plausibility of the proposed mechanism, we first tested the photoreaction in the presence of radical scavenging reagents such as TEMPO and TBHP (Fig. 4a, Fig. S5); however, no significant influence on the reaction progress was observed. We surmised that this is due to the rapid intramolecular cyclization and therefore conducted the radical trapping experiment using non-cyclizing acetophenone oxime ether **8** (Fig. 4b). The photoreaction of **8** in the presence of DMPO revealed the formation of DMPO adduct of acetophenone imine **9** (Fig. S6), indicating that the reaction proceeds *via* iminyl radical intermediate. Furthermore, the possible involvement of O₂ as an oxidizing source was supported by the detection of H₂O₂ in the reaction mixture using the fluorescent probe (Fig. S7). We also attempted the structural determination of the reaction

byproducts, where we expected the sequential formation of compounds **6** and **7**. To this end, **3b** was photo-irradiated for 1 min and analyzed by RP-HPLC (Fig. 4b). The chart showed the presence of two byproducts; structural determination revealed the formation of 4,5-dimethoxy-2-nitrobenzaldehyde **6** and 4,5-dimethoxy-2-nitrosobenzoic acid **7**. These findings demonstrate that the current photocyclization reaction involves the formation of *o*-nitrobenzaldehyde, in contrast to the conventional pathway of *o*-nitrobenzyl deprotection, which would result in the production of *o*-nitrosobenzaldehyde as a byproduct of the photolysis and is consistent with the proposed mechanism in Scheme 2.

(a) Photoreaction in the presence of radical scavengers



(b) Iminyl radical trapping experiment



(c) Determination of the byproducts



Figure 4. Mechanistic studies of the photoinduced intramolecular cyclization reaction. ^a4:1 (v/v) mixture of DMSO-*d*₆ and sodium phosphate buffer (10 mM in D₂O, pH 7.0). Yields were determined by ¹H NMR using maleic acid as an external standard. ^b4:1 (v/v) mixture of DMSO and sodium phosphate buffer (10 mM, pH 7.0).

It should also be noted that the present photoinduced N–O homolysis is highly dependent on the substituents on the *o*-nitrobenzyl moieties (Table 1) or on the presence of an aqueous buffer solution (Table 2). The reasons are currently unclear; however, we deduce that this is due to the enhanced regeneration of the starting material from the *aci*-nitro intermediate (see Scheme S1 and S2 for details). The formation of C–O cleaved compound **5** could theoretically be suppressed by such enhanced reversion reactions, favoring the formation of phenanthridine *via* N–O homolysis.

Lastly, we investigated whether the present reaction proceeds in a cellular environment. We chose the photoinduced cyclization of the biaryl compound **3n** as a model reaction; fluorescence spectroscopic studies showed that the cyclization precursor **3n** barely exhibits the fluorescence signal whereas the corresponding phenanthridine derivative **4n** displays fluorescence in aqueous conditions (Fig. S8). We reasoned that the fluorescence properties of **3n** and **4n** would allow us to monitor the reaction progress inside living cells using fluorescence microscopy measurement. Thus, HeLa cells were incubated with a DMEM solution of **3n** or **4n** (50 μM; 1% DMSO). After exchanging the medium, the cells were treated with and without

the 405 nm LED light and observed with a fluorescence microscope. Fluorescence signals were detected inside the cells when the **4n** was incubated with the cells (Fig. 5a). However, no discernible fluorescence was seen in the cells treated with **3n** in the dark (Fig. 5b). In contrast, the fluorescence signal in the cells appeared after the cells were incubated with **3n** and then exposed to the 405 nm photoirradiation (Fig. 5c). These findings demonstrate that the present photocyclization reaction proceeds inside the living cells, thereby confirming its compatibility with biological environments.

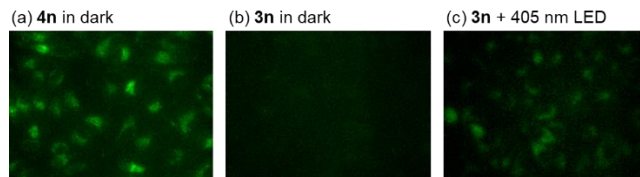


Figure 5. (a) Investigation of biocompatibility of the reaction using **3n** and **4n**. Fluorescence imaging of HeLa cells treated with (b) **4n** in dark, (c) **3n** in dark, and (d) **3n** followed by 405 nm LED irradiation.

In summary, we have demonstrated that *o*-nitrobenzyl oxime ether undergoes photoinduced N–O homolysis and enables the phenanthridine forming intramolecular cyclization reaction. The reaction is initiated upon 405 nm LED light irradiation in aqueous conditions and provides various phenanthridine derivatives with up to 96% yield. Additionally, it was discovered that the reaction is compatible under biological conditions. We believe that by enabling the on-demand photo-construction of *N*-centered heteroaromatics, our findings will open up new avenues for the photochemical control of functional molecules in chemical biology, medicinal chemistry, and material sciences. In our lab, we are currently extending range of the reaction and applying it to the photo-triggered formation of bioactive compounds in a cellular environment.

ASSOCIATED CONTENT

Supporting Information

The Supporting Information is available free of charge on the ACS Publications website.

Experimental details and characterization data of the compounds (PDF)

AUTHOR INFORMATION

Corresponding Authors

Hidenori Okamura – Institute of Multidisciplinary Research for Advanced Materials, Tohoku University, Sendai, Miyagi 980-8577, Japan; Department of Chemistry, Graduate School of Science, Tohoku University, Sendai 980-8578, Japan; Email: hidenori.okamura.b8@tohoku.ac.jp

Fumi Nagatsugi – Institute of Multidisciplinary Research for Advanced Materials, Tohoku University, Sendai, Miyagi 980-8577, Japan; Department of Chemistry, Graduate School of Science, Tohoku University, Sendai 980-8578, Japan; Email: fumi.nagatsugi.b8@tohoku.ac.jp

Authors

Momoka Iida – Institute of Multidisciplinary Research for Advanced Materials, Tohoku University, Sendai, Miyagi 980-8577, Japan; Department of Chemistry, Graduate School of Science, Tohoku University, Sendai 980-8578, Japan

Yui Kaneyama – Institute of Multidisciplinary Research for Advanced Materials, Tohoku University, Sendai, Miyagi 980-8577, Japan; Department of Chemistry, Graduate School of Science, Tohoku University, Sendai 980-8578, Japan

Notes

The authors declare no competing financial interest.

ACKNOWLEDGMENT

This work was supported by the Japan Society for the Promotion of Science (JSPS) Grants-in-Aid for Scientific Research (KAKENHI) (Grants JP21K14749). We thank Daisuke Unabara (Tohoku University) for assistance in NMR measurements.

REFERENCES

1. Mayer, G.; Heckel, A. *Angew. Chem. Int. Ed.* **2006**, *45*, 4900-4921.
 2. Bardhan, A.; Deiters, A. *Curr. Opin. Struct. Biol.* **2019**, *57*, 164-175.
 3. Welleman, I. M.; Hoorens, M. W. H.; Feringa, B. L.; Boersma, H. H.; Szymanski, W. *Chem. Sci.* **2020**, *11*, 11672-11691.
 4. Kaplan, J. H.; Forbush, B., 3rd; Hoffman, J. F. *Biochemistry* **1978**, *17*, 1929-1935.
 5. Hellrung, B.; Kamdzhilov, Y.; Schwörer, M.; Wirz, J. *J. Am. Chem. Soc.* **2005**, *127*, 8934-5.
 6. Yamaguchi, S.; Chen, Y.; Nakajima, S.; Furuta, T.; Nagamune, T. *Chem. Commun.* **2010**, *46*, 2244-2246.
 7. Horbert, R.; Pinchuk, B.; Davies, P.; Alessi, D.; Peifer, C. *ACS Chem. Biol.* **2015**, *10*, 2099-2107.
 8. Smaga, L. P.; Pino, N. W.; Ibarra, G. E.; Krishnamurthy, V.; Chan, J. *J. Am. Chem. Soc.* **2020**, *142*, 680-684.
 9. Brown, W.; Bardhan, A.; Darrah, K.; Tsang, M.; Deiters, A. *J. Am. Chem. Soc.* **2022**, *144*, 16819-16826.
 10. Il'ichev, Y. V.; Schwörer, M. A.; Wirz, J. *J. Am. Chem. Soc.* **2004**, *126*, 4581-4595.
 11. Klan, P.; Solomek, T.; Bochet, C. G.; Blanc, A.; Givens, R.; Rubina, M.; Popik, V.; Kostikov, A.; Wirz, J. *Chem. Rev.* **2013**, *113*, 119-191.
 12. Yong, P. K.; Banerjee, A. *Org. Lett.* **2005**, *7*, 2485-2487.
 13. Qvortrup, K.; Petersen, R. G.; Dohn, A. O.; Moller, K. B.; Nielsen, T. E. *Org. Lett.* **2017**, *19*, 3263-3266.
 14. Talukdar, V.; Vijayan, A.; Kumar, K. N.; Radhakrishnan, K. V.; Das, P. *Adv. Synth. Catal.* **2021**, *363*, 1202-1245.
 15. Tumir, L. M.; Radic S. M.; Piantanida, I. *Beilstein J. Org. Chem.* **2014**, *10*, 2930-2954.
 16. Alonso, R.; Campos, P. J.; Garcia, B.; Rodriguez, M. A. *Org. Lett.* **2006**, *8*, 3521-3523.
 17. Hofstra, J. L.; Grassbaugh, B. R.; Tran, Q. M.; Armada, N. R.; de Lijser, H. J. *J. Org. Chem.* **2015**, *80*, 256-265.
 18. Jiang, H.; An, X.; Tong, K.; Zheng, T.; Zhang, Y.; Yu, S. *Angew. Chem. Int. Ed.* **2015**, *54*, 4055-4059.
 19. Sun, J.; He, Y.; An, X.-D.; Zhang, X.; Yu, L.; Yu, S. *Org. Chem. Front.* **2018**, *5*, 977-981.
 20. Yang, J. C.; Zhang, J. Y.; Zhang, J. J.; Duan, X. H.; Guo, L. N. *J. Org. Chem.* **2018**, *83*, 1598-1605.
 21. Natarajan, P.; Chuskit, D.; Priya, P. *Green Chem.* **2019**, *21*, 4406-4411.
 22. Wan, P.; Yates, K. *Can. J. Chem.* **1986**, *64*, 2076-2086.
-